Environment International 168 (2022) 107474

Contents lists available at ScienceDirect

Environment International

journal homepage: www.elsevier.com/locate/envint

Full length article

Trade-off for survival: Microbiome response to chemical exposure combines activation of intrinsic resistances and adapted metabolic activity

Wisnu Adi Wicaksono [a,*], Maria Braun [b], Jörg Bernhardt [b], Katharina Riedel [b], Tomislav Cernava [a,*], Gabriele Berg [a,c,d,*]

[a] Institute of Environmental Biotechnology, Graz University of Technology, Graz, Austria
[b] Institute of Microbiology, University of Greifswald, Greifswald, Germany
[c] Leibniz-Institute for Agricultural Engineering and Bioeconomy Potsdam (ATB), Potsdam, Germany
[d] Institute for Biochemistry and Biology, University of Potsdam, Potsdam, Germany

ARTICLE INFO

Handling Editor Adrian Covaci

ABSTRACT

The environmental microbiota is increasingly exposed to chemical pollution. While the emergence of multi-resistant pathogens is recognized as a global challenge, our understanding of antimicrobial resistance (AMR) development from native microbiomes and the risks associated with chemical exposure is limited. By implementing a lichen as a bioindicator organism and model for a native microbiome, we systematically examined responses towards antimicrobials (colistin, tetracycline, glyphosate, and alkylpyrazine). Despite an unexpectedly high resilience, we identified potential evolutionary consequences of chemical exposure in terms of composition and functioning of native bacterial communities. Major shifts in bacterial composition were observed due to replacement of naturally abundant taxa; e.g. *Chthoniobacterales* by *Pseudomonadales*. A general response, which comprised activation of intrinsic resistance and parallel reduction of metabolic activity at RNA and protein levels was deciphered by a multi-omics approach. Targeted analyses of key taxa based on metagenome-assembled genomes reflected these responses but also revealed diversified strategies of their players. Chemical-specific responses were also observed, e.g., glyphosate enriched bacterial r-strategists and activated distinct ARGs. Our work demonstrates that the high resilience of the native microbiota toward antimicrobial exposure is not only explained by the presence of antibiotic resistance genes but also adapted metabolic activity as a trade-off for survival. Moreover, our results highlight the importance of native microbiomes as important but so far neglected AMR reservoirs. We expect that this phenomenon is representative for a wide range of environmental microbiota exposed to chemicals that potentially contribute to the emergence of antibiotic-resistant bacteria from natural environments.

1. Introduction

The exposome concept strives to capture the diversity and range of exposures to synthetic chemicals as well as their corresponding biological responses. The term was implemented in 2005 for non-genetic factors influencing health (Wild 2005) and represents a breakthrough on our way to understand the basis of complex diseases (Vermeulen et al. 2020). One of the integral parts of the exposome concept is chemical exposure. To date, studies on the chemical exposome are primarily focused on human health (Vermeulen et al. 2020); however, studies at ecosystem level are urgently needed as well (UNEP 2019). Ecosystem health is substantially affected in the Anthropocene, which is reflected in the planetary boundary concept (Steffen et al. 2015). Recently, novel entities including a wide range of synthetic chemicals were identified as a major problem. This pollution is considered to have already crossed the planetary boundary as annual production and releases increase at a pace that outstrips the global capacity for assessment and monitoring (Persson et al. 2022). Chemical pollutants defined as "new substances, new forms of existing substances and modified life forms", are especially released under intense agriculture, which is therefore a major driver of the Anthropocene (Bernhardt et al. 2017; Persson et al. 2022).

Antibiotics used for intensive livestock farming have been already

* Corresponding authors at: Graz University of Technology, Graz.
E-mail addresses: wisnu.wicaksono@tugraz.at (W. Adi Wicaksono), mariabraun145@gmail.com (M. Braun), joerg.bernhardt@uni-greifswald.de (J. Bernhardt), riedela@uni-greifswald.de (K. Riedel), tomislav.cernava@tugraz.at (T. Cernava), gabriele.berg@tugraz.at (G. Berg).

https://doi.org/10.1016/j.envint.2022.107474
Received 21 April 2022; Received in revised form 11 August 2022; Accepted 12 August 2022
Available online 17 August 2022

banned in many countries but they are still being used in most developing countries in increasing amounts (Van Boeckel et al. 2015). The global use of agricultural pesticides for plant production in 2021 amounted to 4.19 million metric tons; never before in agricultural history have more pesticides been used worldwide than today (FAOSTAT 2021). It is well-established that the use of agrochemicals can contribute to the development of antimicrobial resistance (AMR) in microorganisms (Berendonk et al. 2015; Søgaard Jørgensen et al. 2018). Moreover, AMR is currently recognized as one of the top ten global public health threats (World Health Organization 2021). By 2050, 10 million deaths are predicted to be caused by drug-resistant pathogens; a recent study providing the first comprehensive assessment of the global burden of AMR, showed that already 4.95 million deaths were associated with bacterial AMR in 2019 (Murray et al. 2022). These alarming numbers require an understanding of the role of environmental microbiota in the rise of antibiotic resistance in order to develop innovative counter-strategies (Davies and Davies 2010).

Natural ecosystems often show a high microbial prevalence and diversity and are considered as the main reservoir of AMR genes (Martinez et al. 2009; Martínez 2012) collectively known as the resistome. While *in vitro* population assays with isolated cultures have provided a thorough understanding of antimicrobial activity and resistance mechanisms, bacteria typically coexist in multi-species populations (Berg et al. 2020), and the response of single species is unlikely to be sufficient to determine the degree of the resistance in a defined system (Bottery et al. 2020). Metagenomics-based explorations of complex microbial communities, and especially holistic approaches linking results obtained with different experimental methods, have substantially deepened our understanding related to natural antimicrobial resistance reservoirs including such from the pre-antibiotic era (Martínez 2012; Van Goethem et al. 2018; Berg et al. 2020; Brealey et al. 2020; Obermeier et al. 2021). Nevertheless, there is a lack of mechanistic insights into the evolution of AMR in native microbiomes and their response to chemical exposures. Moreover, understanding the sources of antibiotic resistance genes (ARGs) in isolated natural ecosystems with little anthropogenic influence could improve our understanding of the evolution of resistant pathogens (Van Goethem et al. 2018). Currently, we lack realistic models which can sufficiently represent a complex environmental microbiota that is sensitive toward chemical exposure but also can be manipulated in a controlled environment.

In this study, we implemented the lung lichen *Lobaria pulmonaria* (L.) Hoffm. as a bioindicator organism and model for a native microbiome. Lichens represent multi-species microbial symbioses with an extremely long-lived and resilient life style (Grube et al. 2015; Berbee et al. 2020), and thus provide defined microbial communities to address complex host-microbe interplay and community-level responses to environmental stress (Cernava et al. 2018; Cernava et al. 2019; Wicaksono et al. 2021). Moreover, lichens are widespread in all ecosystems and cover approximately 7 % of the Earth's surface (Ahmadjian 1995). Together with the plant phyllosphere they can be considered as an important source of microorganisms on Earth (Vorholt 2012) but our understanding of the risks associated with their chemical exposure is limited. Lichens, as a classical model of symbiosis, are well suited for the systematic study of the potential evolutionary consequences of chemical exposure to a complex microbial community and complex AMR reservoir.

To systematically examine responses towards chemical exposure, we exposed defined lichen microbiomes to clinical antibiotics, *i.e.*, colistin and tetracycline that are widely applied in agriculture (Collignon et al. 2016; Caniaux et al. 2017; Park et al. 2017) as well as two non-clinical antimicrobial substances, *i.e.*, glyphosate and alkylpyrazine. Colistin is a narrow spectrum antibiotic targeting Gram-negative bacteria by disturbing the integrity of the outer membrane (Li et al. 2006; Paterson and Harris 2016). Tetracycline exhibits activity against Gram-negative and -positive bacteria by blocking the attachment of charged aminoacyl-tRNA at the ribosome's P site peptide chain. Glyphosate was included due to its wide use as herbicide and due to the fact that it may pose a risk factor to promote antimicrobial resistance (Ramakrishnan et al. 2019; Liao et al. 2021) while the employed alkylpyrazine is a newly discovered, non-clinical antimicrobial of bacterial origin with no reports in relation to resistance formation (Kusstatscher et al. 2017; Krug et al. 2019). By combining an integrative multi-omics approach at DNA, RNA, and protein level with complementary 16S rRNA gene amplicon sequencing, we showed that resistance mechanisms in a native microbiome towards antimicrobial compounds include activation of intrinsic resistances and adapted metabolic activity as a trade-off for survival. This study provides important insights into mechanisms of AMR evolution in a native ecosystem and can be used to develop AMR management strategies in the future.

2. Methods

2.1. Lichen material and antimicrobial treatment

L. pulmonaria thallus samples were collected from a rich population on maple tress (*Acer pseudoplatanus* L.) in the Austrian Alps (N47.6124 E14.8359). Macroscopic contaminations, *i.e.*, moss and bark were removed with sterile tweezers. Following the initial pre-processing steps, lichen thalli (1.5 g dry weight) were placed in sterile Petri dishes. Four different antimicrobials were implemented including colistin sulfate (Sigma-Aldrich, USA), tetracycline (Merck, Germany), glyphosate (commercial herbicide Roundup® Alphée containing glyphosate at 7.20 g/l, Scotts Celaflor, Mainz, Germany), and an antimicrobial alkylpyrazine (5-isobutyl-2,3-dimethylpyrazine 97 %; Sigma-Aldrich, USA). Two concentrations of each antimicrobial compound in aqueous working solutions that represent the full dosage (FD) and a reduced dosage (1/10 dilution of FD) were prepared in sterile water. In total, eight different treatments were used to expose the lichen microbiota to the antimicrobials (Table S1). The full dosage was determined based on previous studies (Mbanaso et al. 2013; Ye et al. 2015; Semedo et al. 2018; Krug et al. 2019) that assessed the optimal concentration of each compound based on oral administration in animals or efficacy assessments in other test systems (Table S1).

Lichen thalli were separately exposed to each compound every 24 h over a period of 10 days by spray application of the solutions (approximately 1.5 mL per treatment) on confined lichens. Controls were obtained by applying sterile water without antimicrobial compounds. During the treatment period all samples were kept in the laboratory at room temperature. Each treatment was performed with three biological replicates. Following the 10-day exposure, all samples were transferred into 15-ml Sarstedt tubes prefilled with RNAlater (Ambion, Life Technologies, Germany) stabilization solution (for total nucleic acid extraction) and empty tubes (for protein extraction) and stored in −80 °C until further use.

2.2. Nucleic acid extraction and cDNA synthesis

Total community DNA and RNA were isolated from approximately 100 mg of lichen thallus samples, using the FastDNA™ SPIN Kit for Soil (MP Biomedicals) and TRIzol® Plus RNA Purification Kit (Ambion, Life Technologies), respectively, following the manufacturer's instructions. The RNA and DNA quality and quantity were measured by using a NanoDrop™ 2000/2000c spectrophotometer together with the Qubit dsDNA BR and Qubit RNA HS Assay Kit (ThermoFischer Scientific), respectively. Subsequently, the RNA integrity was assessed using the Qubit RNA IQ Assay (ThermoFischer Scientific) to assure sufficient quality before further processing. Total RNA (100 ng) was used to synthetize cDNA using 5X All-In-One RT MasterMix (Applied Biological Materials, Richmond, BC, Canada) according to the manufacturer's instructions. The obtained cDNA was diluted 10 times prior to amplification of marker genes for quantitative PCR (qPCR) and amplicon library construction.

2.3. Bacterial quantification in lichen samples

Using the primer pair 515f/927r, quantitative real-time PCR (qPCR) based on SYBR Green fluorescence was used to assess the total and active bacterial density after antimicrobial exposures. The qPCR mix contained 1 μL DNA/cDNA template, 5 μL KAPA SYBR® FAST qPCR Master Mix (2X) (KAPA Biosystem, USA), 1 μL 10 μM of each primer, and 3 μL ultrapure water. Fluorescence quantification was done using the Rotor-Gene 6000 real-time rotary analyser (Corbett Research, Sydney, Australia).

2.4. Amplicon sequencing of active and total microbial communities

Extracted DNA and cDNA were subjected to PCR-based barcoding using the primer set 515f/926r to target the V4-V5 region of the bacterial 16S rRNA gene (Parada et al. 2016). PCR products were visualized on 1 % agarose gels to verify amplification and subsequently purified using the Wizard® SV Gel and PCR Clean-Up kit (Promega). After pooling all barcoded amplicons in equimolar concentrations, the samples were sent to the commercial sequencing provider Genewiz (Leipzig, Germany) for library preparation and sequenced on the Illumina MiSeq platform (2 × 300 bp paired-end reads).

2.5. Total community RNA sequencing

To enrich the mRNA fraction from the total RNA samples, we employed a subtractive hybridization approach via sample-specific biotinylated rRNA probes according to a previous study (Stewart et al. 2010). We implemented metagenomic DNA to construct specific biotinylated rRNA probe sets that target prokaryotic and eukaryotic SSU and LSU rRNA. Probe construction and removal of rRNA were performed as previously described by (Cernava et al. 2019). rRNA-depleted samples were subjected to strand-specific RNA library preparation and metatranscriptomic sequencing was conducted on an Illumina HiSeq 2500 instrument (2 × 150 bp paired-end reads) by the sequencing provider Genewiz (Leipzig, Germany).

2.6. Bioinformatic analyses of DNA and RNA datasets

We used the open-source pipeline QIIME2 version 2019.10 (https://qiime2.org(Bolyen et al. 2019)) to perform microbial community analyses based on amplicon sequences. The reads were quality filtered, trimmed, denoised, and merged with the implemented DADA2 algorithm (Callahan et al. 2016) followed by removal of chimeric sequences. The obtained bacterial sequence variants (ASVs) were taxonomically classified by using the VSEARCH classifier (Rognes et al. 2016) based on the reference database Silva v128 (Pruesse et al. 2007). Prior to further analysis, all reads assigned to chloroplasts, mitochondria as well as sequences assigned to the genus *Nostoc* were removed, because it occurs spatially segregated as second photobiont of the lung lichen; therefore, these sequences were not considered as part of the microbiome. The final dataset contained 3.34×10^5 ($6{,}17 \times 10^3$ per sample mean) of bacterial reads that were assigned to 1169 bacterial ASVs.

To construct functional profiles, a metagenomic dataset that was previously published (Grube et al. 2015) and obtained from the same lichen population, was re-analysed with updated bioinformatic tools and then served as reference database for mapping metatranscriptomic data. First, the Illumina adaptors were removed and filtered raw reads were obtained using Trimmomatic and VSEARCH (Bolger et al. 2014; Rognes et al. 2016). The high-quality reads were *de novo* assembled using metaSPAdes with defaults parameters (Nurk et al. 2017). Taxonomic composition based on protein-level sequence classification was performed with Kaiju (Menzel et al. 2016). Assembled contigs were then annotated using the blast algorithm in DIAMOND against the eggNOG database 5.0 (Huerta-Cepas et al. 2019) to reveal ecologically relevant functional subsystem. Assembled contigs were additionally annotated with the manually curated antibiotic resistance gene database (deepARG,(Arango-Argoty et al. 2018) to obtain antibiotic resistance gene (ARG) profiles. To minimize the risk of false-positives, reads were defined as ARG-like reads at the cutoff *E* value of 10^{-10} and similarity of 35 % as previously described by (Looft et al. 2012). All reads that fulfilled these parameters were considered to contain the biomolecular machinery required for antibiotic resistance. To get insight into potential horizontal gene transfer (HGT) after the event of antimicrobial exposures, we first searched putative plasmid contigs that carried ARGs using Plasflow (Krawczyk et al. 2018) and other mobile genetic elements, *i.e.*, transposon, integron and insertion elements using custom mobile genetic element as described previously (Liu et al. 2019). Antibiotic resistance genes were considered mobile if they shared a contig with a mobile genetic element.

For metatranscriptomic sequence analysis, the reads were quality filtered as described above resulting in a total of 263.6 Gbp (giga base pairs) high-quality reads. As rRNA was not completely removed during the molecular enrichment of the mRNA fraction, we identified and removed the remaining rRNA reads by aligning them against SILVA and Greengenes rRNA databases (Pruesse et al. 2007; McDonald et al. 2012) using the Burrows-Wheeler Alignment tool (Li and Durbin 2010). Between 64.2 and 77.9 % of the total reads were identified as non-rRNA reads (Supplementary Table S2). Bowtie2 (Langmead and Salzberg 2012) and FeatureCounts (Liao et al. 2014) were used to align metatranscriptomic sequences individually to annotated contigs derived from the metagenomic dataset and to obtain read numbers, respectively. Only those reads that mapped to contigs with eggNOG and deepARG annotations were used for further analyses. A total of 3.84×10^8 ($1{,}42 \times 10^7$ per sample mean) and 4.57×10^5 ($1{,}69 \times 10^4$ per sample mean) metatranscriptomic reads were retained and annotated using eggNOG and deepARG databases, respectively.

Genome binning from the metagenomic dataset was performed using Maxbin2, MetaBAT2 and CONCOCT (Alneberg et al. 2014; Wu et al. 2016; Kang et al. 2019) and then de-replicated and aggregated into metagenome-assembled genomes (MAGs) using DASTool (Sieber et al. 2018). Completeness and the percentage of contaminants in the MAGs were estimated by using CheckM (Parks et al. 2015). Only MAGs with a completeness of 75 % and contamination < 5 % were selected for further analyses. MAGs were taxonomically classified using the Bin Annotation Tool (BAT, (von Meijenfeldt et al. 2019)). MAGs representing the order *Chthoniobacterales* were not recoverable from the datasets, thus we decided to construct a *Chthoniobacter* pangenome by using publicly available genome sequences of *Chthoniobacter flavus* Ellin428 and *Chthoniobacter flavus* DSM 22,515 to represent this dominant bacterial group in lichens. The pangenome was constructed by using Panseq, a web server for bacterial pan-genome analysis (Laing et al. 2010). Open reading frames of each MAG were predicted using Prodigal and functional annotation was performed using eggNOG mapper (Hyatt et al. 2010; Huerta-Cepas et al. 2017). Quantification of expressed genes was performed using the Burrows-Wheeler Alignment and FeatureCounts (Li and Durbin 2010; Liao et al. 2014) as described above.

2.7. Metaproteomics

For metaproteomic analyses, we extracted proteins from three technical replicates of the control samples, the full-dosage colistin treatment, and the full-dosage alkylpyrazine treatment. Total proteins were extracted according to an adapted extraction protocol (Wang et al. 2006). Protein gel electrophoresis and in-gel digestion after SDS-polyacylamide gel electrophoresis were performed as previously described (Grube et al. 2015) with a slight modification (Method S1).

The obtained peptide mixtures from three technical replicates of each sample were analyzed by GeLC − MS/MS using an Orbitrap Elite mass spectrometer (Thermo Scientific, Waltham, MA). The raw files were converted to MGF files by MSConvert (version 1.0.98, ProteoWizard). Mass spectra of all samples were searched in the next steps against

a compiled database including a partly translated metagenome of *L. pulmonaria*. The converted raw files were searched with the Mascot search engine (version 2.7.0, Matrix Science, London, U.K.) with the following parameters: peptide tolerance 10 ppm, MS/MS tolerance 0.6 Da, maximum missed cleavages 2, charge state 2+, 3+, 4 + and oxidation of methionine as variable modification. Scaffold (version 4.11.0, Proteome Software, Portland, OR, USA) was used to validate MS/MS-based peptide and protein identifications. Scaffold analysis was performed as a "MudPit experiment" to merge the individual mascot result files into a single data set. The metaproteome analyses pipeline Prophane 2.0 (https://www.prophane.de) was implemented for functional classification and phylogenetic distribution of the assigned proteins (Schiebenhoefer et al. 2020). Proteins were clustered based on the shared peptide spectrum matches (PSMs). One master protein represents each protein cluster (or protein group). The master protein was selected based on PSM coverage and probability scores. Relative protein quantification was based on normalized spectral abundance factor (NSAF) values (Table S3).

2.8. Statistical analyses

R software (https://www.r-project.org) was used for conducting statistical analyses and creating the corresponding graphs unless stated otherwise. Significant differences of bacterial gene copy numbers were analysed using the non-parametric Kruskall-Wallis test. For microbial community analysis, the ASV tables and taxonomic classifications were imported into R via phyloseq and MicrobiomeAnalyst (McMurdie and Holmes 2013; Chong et al. 2020). We normalised the amplicon sequencing library by randomly selecting subsets of sequences according to the lowest number of read counts in a single sample of the set. A taxonomy summary was obtained for the top 100 most abundant ASVs at class level. Differences in microbial alpha diversity based on the Shannon index were analysed using the Kruskal Wallis test. The beta diversity, based on the normalized Bray-Curtis dissimilarity matrix, was subjected to permutational analysis of variance (PERMANOVA, 999 permutations) to test for significant effects of experimental factors on microbial community structures. The distance matrices were visualized by using principal coordination analysis (PCoA) through the R package vegan (Oksanen et al. 2007). Circle packing diagram was generated using rawgraphs (https://rawgraphs.io/). DESeq2 analysis (Love et al. 2014) was performed in order to examine differences in relative proportions of abundant taxa between treated samples and the control ($P_{adjusted}$ value after the B-H adjustment < 0.1 and log2fold change value > 1). Finally, correlation network analysis was conducted to explore the bacterial interactions at order level. Only $P_{adjusted}$ values<0.05 and Pearson's correlation coefficients higher than 0.8 were included in the networks.

For comparative metatranscriptomic analysis, the output read count tables were used as an input for DESeq2 for data normalisation and differential expression analysis (Love et al. 2014). Genes were collapsed to COG categories and their abundances were visualized using bar plots. For differential expression analysis, we removed low count genes (<10 reads) to improve the sensitivity of the differential gene expression analysis. DESeq2 analysis was then used to obtain a list of differentially expressed genes after the BH adjustment ($P < 0.1$, default cut off suggested by DESeq2 (Love et al. 2014) in pairwise comparisons between control and each antibiotic treatment. We corrected the normalized metatranscriptomic abundance profiles using a regularized logarithm - transformation as implemented in the DESeq2 R package (Love et al. 2014). To allow construction of the Bray-Curtis matrix distance, the negative values from the normalized dataset were replaced with a zero under the assumption that negative values represent very low or zero abundance and thus are of negligible importance for the hypotheses. The normalized Bray-Curtis dissimilarity matrix, subjected to permutational analysis of variance (PERMANOVA, 999 permutations), was then implemented to test for significant effects of antibiotic treatment on microbial functions. Differences in expressed ARG diversity based on the Shannon diversity index were analysed using the Kruskal Wallis test. Uneven sequencing depth was normalized by rarefying each sample to the lowest number of read counts in a single sample of the set. In addition, amplicon sequencing data was correlated to functional profiles. The normalized and rlog-transformed ecological function profiles (eggNOG annotation) and antibiotic resistance gene profiles (deepARG annotation) from metatranscriptomic data were correlated through partial Mantel tests (corrected for spatial distance) with 999 permutations.

For comparative metaproteomic analysis, the log2-transformed ratios of the averaged protein specific NSAF values of at least two of three replicates were used at first as basis for area-size-encoded data visualization of the taxonomical composition of the bacterial community by Voronoi treemaps using the Paver software 2.0 (Decodon; Greifswald, Germany). The cell sizes of each phylogenetic category correspond to the average of the sums of respective normalized NSAF values over all treatments. An adapted colour gradient was used to depict the taxonomical changes in the bacterial microbiome between the control and the colistin or alkylpyrazine treatment. In addition, the log2 transformed ratios and the relative abundance of the averaged protein specific NSAF values of at least two of three replicates were used as a basis for a heatmap showing the changes of specific functions of the bacterial microbiome between the control and the colistin or alkylpyrazine treatment. P-values were calculated with the Multiple Experiment Viewer 4.9.0 (MeV) software. The relative abundances of the averaged protein-specific NSAF values of each replicate were compared using the Wilcoxon rank sum test as the data was not normally distributed and homogeneous in variance.

3. Results

3.1. Antimicrobial exposure had no significant impact on bacterial abundance and diversity suggesting high resilience

After exposure to defined antimicrobial compounds - colistin, tetracycline, alkylpyrazine, glyphosate - over a 10-day period, *L. pulmonaria* phenotypes were differently affected. We observed a phenotypic change of the *Lobaria* thalli in response to the full dosages of glyphosate and alkylpyrazine (Fig. S1). A change of colour from green to dark brown of lichen samples was observed on the 7th day and became more pronounced after the 8th day of continuous exposure. These antimicrobials are primarily targeting the photobiont, the green alga *Symbiochloris reticulata*. Interestingly, lichen thalli that were treated with subtherapeutic dosages of the antimicrobial compounds did not show any distinct phenotypic change in comparison to the control during the whole experiment.

We first assessed the impact of antimicrobial exposure on the bacterial abundance and diversity. Total (per isolated ng DNA) and active (per isolated ng RNA) bacterial counts in untreated samples were determined as 1.64×10^7 and 4.53×10^4 16S rRNA (gene) copies, respectively (Table S4). Despite the variation, antimicrobial exposures did not significantly affect total and active bacterial abundance ($P = 0.119$ and $P = 0.316$, respectively). Interestingly, exposure to different antimicrobials and dosages did not have significant effects on the total ($P = 0.352$ for antimicrobial type and $P = 0.922$ for dosage; Table S5 and Table S6) and active bacterial diversity ($P = 0.721$ for antimicrobial type and $P = 0.204$ for dosage; Table S5 and Table S6). Taken altogether, at the community level, the bacterial abundance and diversity was relatively maintained. Our findings suggest high bacterial community resilience after the continuous exposure even with the full dosage of antimicrobial compounds.

3.2. Antimicrobial exposure substantially affected bacterial community structure and induced abundance shifts within prevalent microbiome members

Antimicrobial exposure significantly affected the total ($P = 0.001$; $R^2 = 0.238$) and active ($P = 0.001$; $R^2 = 0.248$) bacterial community structure. For a better visualisation, PcoA plots were constructed for each of the two antimicrobial dosages while differentiating between the total and active community (Fig. 1A-B and D-E, Table S7). The interaction between antimicrobials and their dosages also affected the bacterial composition, which explained 22.6 and 16.7 % of the bacterial variation in the total and active bacterial community respectively ($P =$

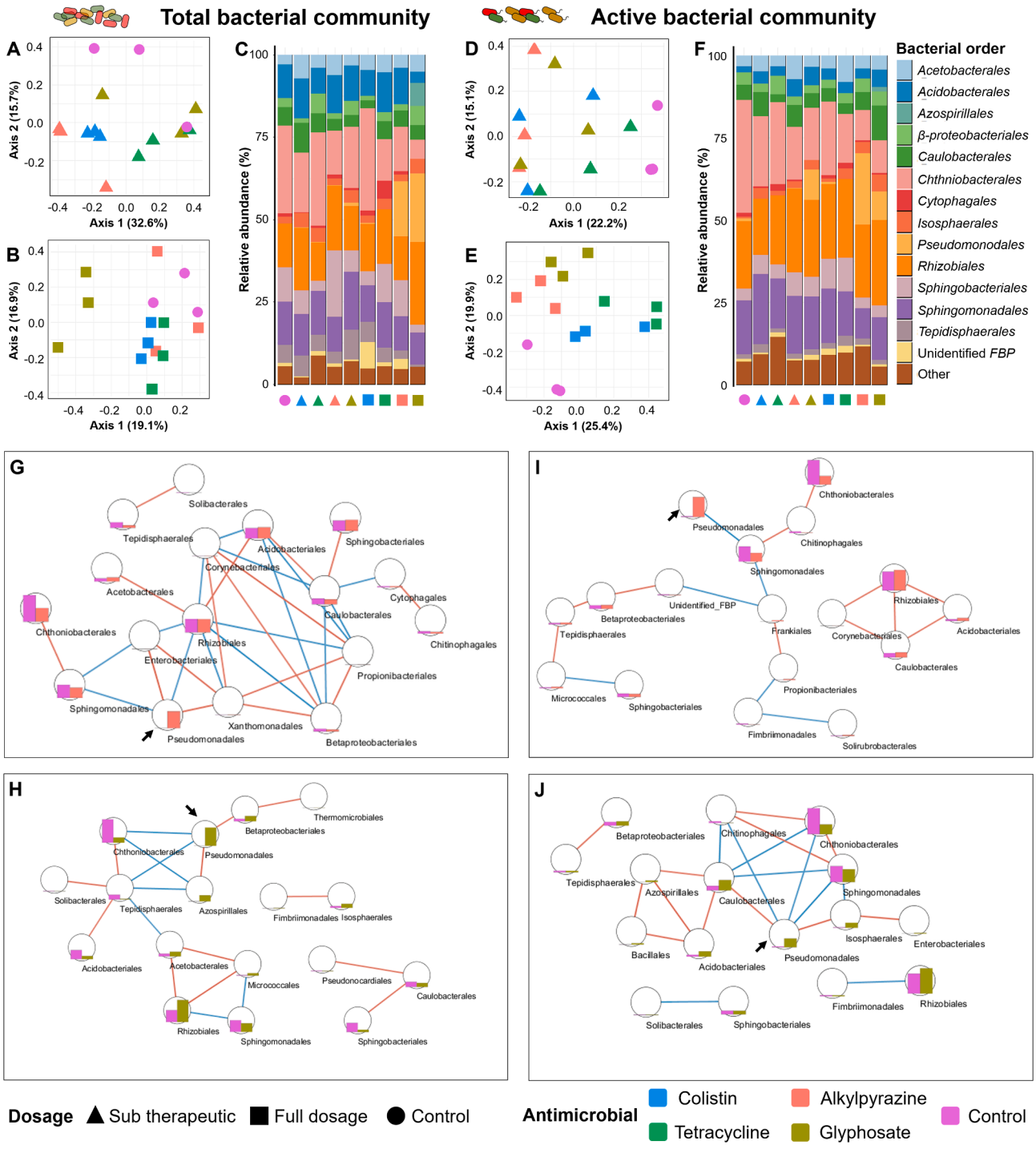

Fig. 1. Responses of the bacterial community structure after 10 days of continuous exposure to antimicrobials. Community clustering and taxonomic composition on order level of total (A, B and C) and active (D, E and F) bacteria. Clustering and composition of bacterial communities in *Lobaria pulmonaria* treated with different antimicrobial substances are visualized in PcoA plots and bar plots respectively. A correlation network analysis (Pearson's correlation) was used to identify shifts in the total (G and H) and active (I and J) bacterial community after 10 days of exposure to alkylpyrazine (G and I) and glyphosate (H and J). Red lines indicate positive correlations and blue lines indicate negative correlations. The arrows indicate that the relative abundance of *Pseudomonadales* increased along a reduction of predominant taxa, e.g., *Sphingomanadales* and *Chtoniobacterales*. (For interpretation of the references to colour in this figure legend, the reader is referred to the web version of this article.)

0.001). The antimicrobial type was shown to be the dominant factor that influences community clustering (Fig. 1A-B and D-E, $P_{adj} < 0.05$). The performed Mantel test indicated that total and active bacterial community structure were significantly correlated ($P < 0.001$, r = 0.335) suggesting a moderately congruent pattern and some overlapping responder taxa between the two approaches. Overall, we observed that antimicrobial exposures induced specific responses on the bacterial community level.

Given the observed changes in the bacterial community structures, we were interested in identifying specific taxonomic groups that responded to the antimicrobial exposure. In untreated samples, six bacterial orders, namely *Chthoniobacterales*, *Rhizobiales*, *Sphingomonadales*, *Sphingobacteriales*, *Acidobacteriales* and *Caulobacterales* were predominant (79.5 - total bacterial fraction and 81.3 % - active bacterial fraction, respectively; Fig. 1C and 1F). We identified bacterial taxa that increased (termed as "positive responders") and declined (termed as "negative responders") in response to the antimicrobial exposures. A DeSeq2-based analysis was used to identify bacterial orders with significantly different abundance between the control and the different antimicrobial treatments. RNA-based community profiling indicated that *Acidobacteriales* increased in response to the full dosage exposure to colistin (3.5 %, respectively) in comparison to untreated samples (2.1 %, Table S9). The relative abundance of *Acidobacteriales* and other prevalent taxa, *i.e.*, *Sphingobacteriales* also increased (3.8 and 10.4 %) in response to full dosage exposure to tetracycline. However, no significant changes were observed by using DNA-based bacterial community profiling for the same comparison indicating variations in the relative proportions of certain taxa between those approaches (Table S8). *Rhizobiales* were also among the dominant taxa that showed resilience after being exposed to the full dosage of colistin, tetracycline, and glyphosate (Table S8 and S9).

Despite the variations, the relative abundance of the most prevalent taxonomic group *Chthoniobacterales* showed a tendency to decrease in treated samples especially with alkylpyrazine and glyphosate. The relative abundance of *Chthoniobacterales* decreased from 26.8 % and 34.6 % to 6.4 % and 10.4 % in the total and active bacterial community, respectively after exposure to the full dosage of glyphosate ($P_{adjusted} < 0.05$; Supplementary Table S8 and Table S9). The relative abundance of *Chthoniobacterales* in the active bacterial fraction was also significantly reduced ($P_{adjusted} = 0.046$, Supplementary Table 9) to 8.8 % after exposure to the full dosage of the alkylpyrazine. Most remarkably, exposure to the antimicrobial alkylpyrazine and glyphosate resulted in a significant increase of *Pseudomonadales* that are naturally a low-abundant taxon in the lichen microbiome which accounted for 9.3–21.7 % of the total and active bacterial community. Encouraged by these results, we performed a correlation network analysis and observed that the enrichment of the positive responder, namely *Pseudomonadales*, is associated with a reduction of *Sphingomonadales* and *Chthoniobacterales* in samples treated with alkylpyrazine and glyphosate (Fig. 1G-1 J). A similar pattern was observed for tetracycline-treated samples, where a reduction of *Chthoniobacterales* was followed by enrichment of rare taxa (<0.01 % of relative abundance) namely *Armatimonadales* and *Micrococcales*. Hence, we observed that the antimicrobial compounds substantially affected the prevalent bacterial taxa and resulted in a bloom of naturally rare taxa.

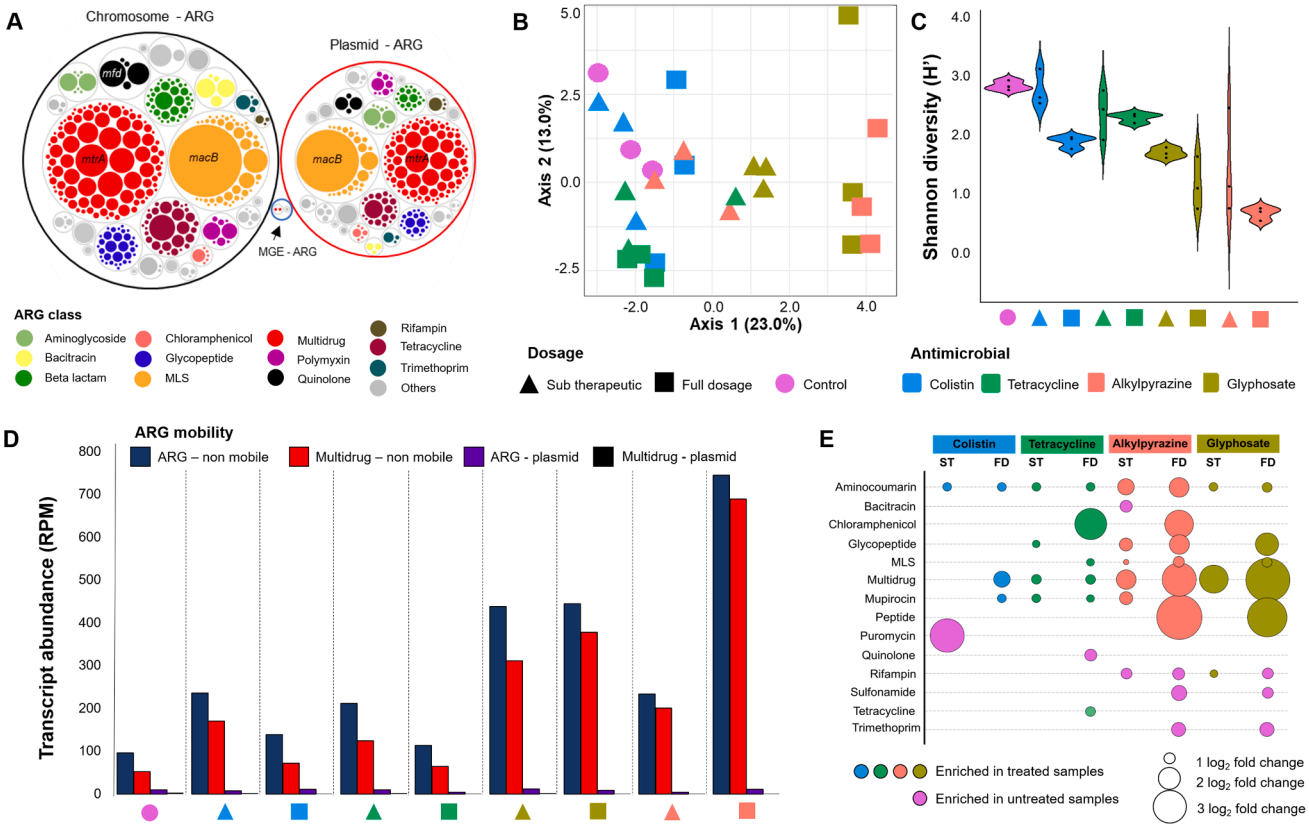

Fig. 2. Antimicrobial resistance genes (ARGs) in the Lobaria microbiome. The overall resistome composition (A) and the diversity of expressed ARGs (B and C) in lichen thalli treated with different antimicrobial substances were assessed. Plasflow was used to predict antibiotic resistance genes located in plasmid contigs, mobile genetic element contigs or chromosomal contigs from assembled metagenome contigs (A). The resistome profile is based on the metagenomic dataset; it was obtained by specific assignments within the deepARG database (A). Different colours indicate specific ARG classes. Beta diversity was assessed with a Bray-Curtis distance matrix of metatranscriptomic samples and visualized in a Principal coordinate analysis (PCoA) plot. Alpha diversity was estimated using the Shannon index. Number of antimicrobial resistance gene transcripts (normalized to reads per million - RPM) that are either mobile or non-mobile in response to antimicrobial exposures (D). Differentially expressed antimicrobial resistance genes in response to antimicrobial exposures according to DeSeq2 analyses (E).

3.3. The lichen comprises a highly diverse resistome dominated by multidrug resistance genes

Using the lichen metagenome as reference dataset, we evaluate the antimicrobial resistance potential of the lichen microbiota. We observed that 0.6 % of the total reads were assignable to 4783 contigs that were classified as ARGs with a frequency between 2.2 and 37678.2 ppm. Among them, 1633 contigs (34.1 %) were connected to plasmids whereas only three contigs were connected to other mobile genetic elements (Fig. 2A). The total antibiotic resistance gene pool comprised 26 antibiotic classes. Multidrug and macrolide-lincosamide-stretogramin (MLS) were the most dominant antimicrobial classes which accounted for 44.2 % of total detected ARGs (Fig. 2A). It is also noteworthy to mention that several genes that specifically confer resistance to rifampin (*iri*, *rphA* and *rphB*), fosfomycin (*murA*), colistin (*mcr-1*), erythromycin (*msrA* and *msrE*) and vancomycin (*vanSA* and *vanB*) were detected. A major proportion (46 %) of the ARGs originated from the phylum *Proteobacteria,* i.e., *Alphaproteobacteria* (*Sphingomonadales* and *Rhizobiales*) and 14 % to *Beta*/Gammaproteobacteria. This finding indicated that the lichen resistome is mainly carried by its naturally prevalent bacterial taxa.

3.4. The lichen microbiome responded by an activation of its intrinsic AMR repertoire where multidrug resistances are naturally prevalent

The focus of the study was on the activation of ARGs that are part of the natural resistome by chemical exposure with resistance-inducing potential. Based on the metatranscriptomic data, we constructed a distance matrix for ARGs based on the Bray-Curtis dissimilarity index and calculated the Shannon diversity index that was used as a proxy for composition (β-diversity) and richness (α-diversity) of the expressed ARGs. Antimicrobial treatments and their dosages substantially affected the composition ($P = 0.001$, $R^2 = 0.589$ and $P = 0.011$, $R^2 = 0.090$, respectively; Fig. 2B) and richness ($P < 0.001$ and $P = 0.002$, respectively; Fig. 2C) of expressed ARGs. Interestingly, we observed a decrease of the expressed ARG richness in the samples treated with antimicrobial compounds, especially glyphosate and the alkylpyrazine, when compared to the control (Fig. 2C). These findings suggest that the lichen microbiome responded toward antimicrobial exposures by selectively expressing certain ARGs that needed to counter the antimicrobial pressure.

Despite a high proportion of ARGs that were associated with plasmids, we observed a strong tendency that non-mobile ARGs showed higher transcriptional activity than mobile ARGs (Fig. 2D). Transcript abundances of total non-mobile ARG and non-mobile multidrug resistance genes were significantly higher in treated samples ($P = 0.007$). However, transcript abundances of total mobile ARGs and mobile multidrug resistance genes between treatments were not statistically different ($P = 0.988$ and $P = 0.088$) indicating that non-mobile ARGs were more actively involved than the mobile ARG in bacterial defence during antimicrobial exposures.

Comparative DeSeq2 analysis of antimicrobial resistance gene classes revealed that genes that were assigned to the multidrug resistance class were significantly upregulated (Table S10) under full dosage exposure to antimicrobial substances when compared to untreated samples ($P < 0.05$; Fig. 2E). Moreover, expressions of genes that were assigned to glycopeptide and peptide resistance classes were also enriched in full-dosage-exposed alkylpyrazine and glyphosate samples in comparison to other treated samples, indicating distinct responses to these antimicrobials. At a deeper level, we identified that the genes that confer multidrug resistance were assigned to resistance-nodulation-cell division (RND), small multidrug resistance (SMR), major facilitator superfamily (MFS) and ATP-binding cassette (ABC) antibiotic efflux pump. Most of them were derived from prevalent members of the lichen microbiota, namely *Rhizobiales* (18 %), *Sphingomonadales* (13 %), *Acidobacteriales* (12 %), *Burkholderiales* (9 %), *Planctomycetales* (5 %), and *Rhodospiralles* (4 %). Detailed analyses indicated that RND antibiotic efflux pumps were highly upregulated in untreated control samples when compared to most of the treated samples; exceptions were found for samples treated with sub-therapeutic dosages of colistin whereas MFS and/or ABC antibiotic efflux pump showed the opposite pattern ($P < 0.05$; Table S11). Only the enrichment of *abcA* and *Mdr* genes was found to be statistically significant after *P* value adjustment (Table S11). We found strong indications that multidrug resistance genes, in particular ABC and MFS antibiotic efflux pumps, are employed by the lichen microbiome as a general response to exposure to antimicrobials with broad-spectrum activity, *i.e.*, glyphosate and the alkylpyrazine.

3.5. Community-level metabolic adaptation in response to antimicrobial exposures

In addition to the activation of the intrinsic resistome, we were also interested in potential metabolic adaptation which might contribute to the microbial community resilience. Function-based clusters in PCoA plots indicated substantial differences between treated and untreated samples (Fig. 3A) as well as antimicrobial with different spectrum activity. Adonis analysis confirmed significance of the observed clusters according to the antimicrobial type ($R^2 = 0.301$; $P = 0.001$), dosage ($R^2 = 0.144$; $P = 0.001$) and the interaction ($R^2 = 0.134$; $P = 0.001$). By employing the Mantel test, we observed a strong association between metabolic function and active bacterial community profiles ($P = 0.001$; $r = 0.404$). Moreover, we also found a strong correlation between metabolic functions and ARG profiles ($P = 0.001$; $r = 0.759$). We suggest that bacterial community changes and their resilience towards antimicrobial exposures are not only tightly connected with activation of intrinsic resistome profiles but also adaptations of metabolic function at community level.

DeSeq2 analyses indicated that the lichen microbial community decreased basal metabolic activity when exposed to the antimicrobial compounds. In comparison to untreated samples, genes that were assigned to key metabolic functions such as energy production and conversion, carbohydrate transport and metabolism, inorganic ion transport and metabolism, and cell wall membrane envelope biogenesis were significantly decreased in treated samples especially in those treated with the full dosages ($P_{adjusted} < 0.05$; Table S12, Fig. 3B). In contrast, the relative abundance of genes assigned to secondary metabolite biosynthesis, transport and catabolism, and defence mechanisms were more expressed especially in samples treated with the full dosage of glyphosate and the alkylpyrazine (Table S12). We found that between 6 and 32 % of the differentially expressed genes (DEGs) were assigned to bacteria (Figure S2 and S3).

We extended our analysis by grouping the differentially expressed genes according to the host origin (bacterial order) to investigate if different bacterial phylogenies show distinct responses toward antimicrobial exposures. Among the downregulated DEGs with $\log_2$ fold change > 2 ($n = 1944$), a high number was assigned to the order *Chthoniobacterales* ($n = 464$), *Rhizobiales* ($n = 358$) and *Sphingomonadales* ($n = 103$). On the other hand, among the upregulated DEGs with $\log_2$ fold change > 2 ($n = 216$), a high proportion was assigned to naturally low abundant taxa, e.g., *Pseudomonadales* ($n = 42$), *Micrococcales* ($n = 12$), *Burkhoderiales* ($n = 11$), *Myxococcales* ($n = 9$), and *Micrococcales* ($n = 12$). The number of DEGs showed a clear upward trend with colistin < tetracycline < alkylpyrazine < glyphosate (Table S13) indicating a more pronounced impact of the non-clinical antimicrobial substances compared to the clinical substances in particular the full dosage exposure.

We found genes that are related to bacterial metabolic functions were likely involved in common responses towards antimicrobial exposure. A decrease in the expression of genes that are related to post-translational modification, protein turnover, chaperones such as heat shock proteins and chaperonin, were observed with naturally abundant members of the microbiome, *i.e.*, *Chthoniobacterales*, *Rhizobiales* and

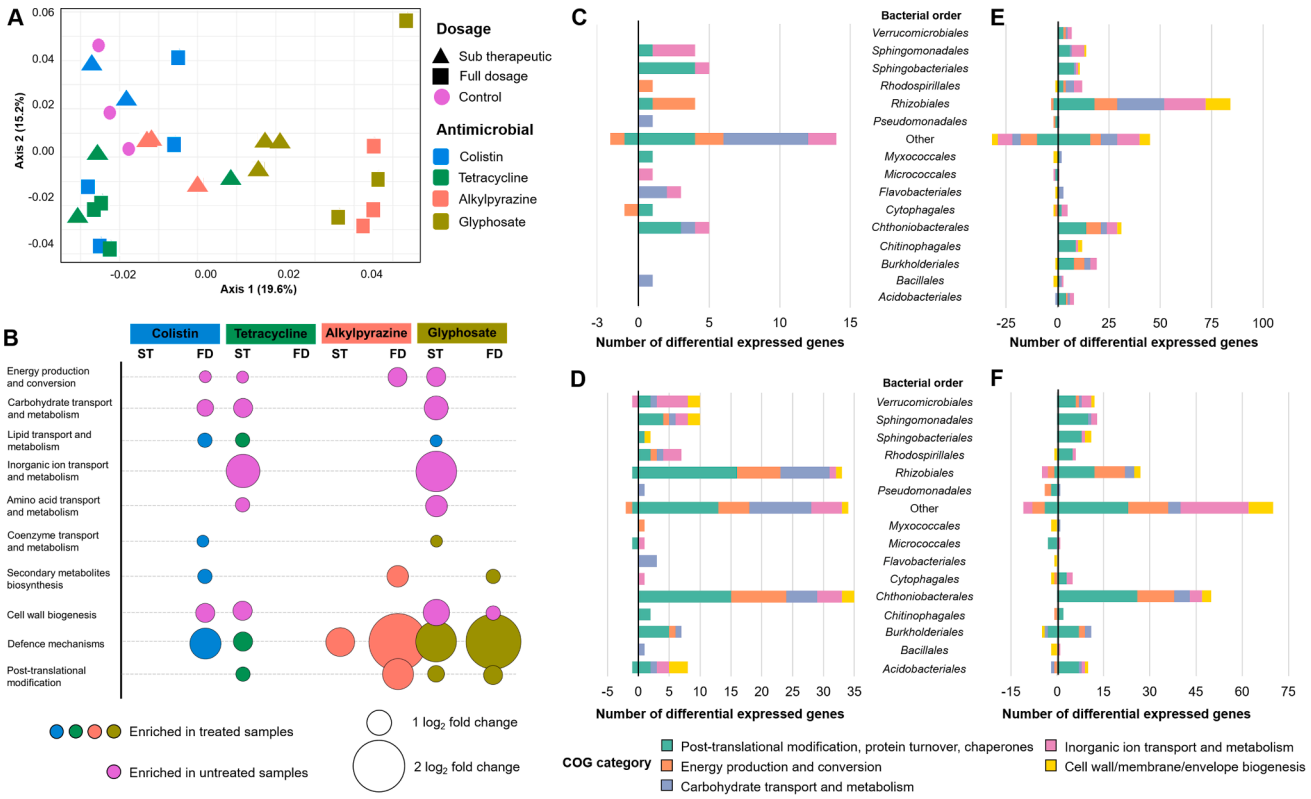

Fig. 3. Comparison of functional assignments of the lichen microbiome and differentially expressed bacterial genes in response to antimicrobial exposures based on metatranscriptomic analysis. A Bray-Curtis distance matrix between samples was visualized using a principal coordinate analysis (PCoA) plot (A). Expressed genes were assigned to Clusters of Orthologous Group (COG) functional categories (B-F). DeSeq2 analysis results show Clusters of Orthologous Group (COG) functional categories that were differentially expressed between the treated samples in comparison to untreated samples (B). Bacterial genes that were differentially expressed under full-dosage treatments with colistin (C), tetracycline (D), glyphosate (E), and alkylpyrazine (F) in comparison to untreated samples were assigned to corresponding bacteria at order level for the identification of prevalent responders. For bar plots (C-F), negative values indicate the number of genes that was enriched in treated samples whereas positive values indicate the number of genes that was enriched in untreated samples.

Sphingobacteriales (Fig. 3C-F). Various DEGs encoding proteins for energy production and conversion, e.g., cytochrome *c* class I and FoF1-type ATP synthase, were also downregulated particularly in samples treated with non-clinical antimicrobials. In contrast, *Pseudomonadales* increased expression of genes encoding succinate dehydrogenase. Within the inorganic ion transport and metabolism gene category, naturally abundant taxa, *i.e.*, *Chthoniobacterales*, *Sphingomonadales*, *Sphingobacteriales*, *Acidobacteriales,* and *Rhizobiales* showed a consistent pattern of reduced expression of ferritin-like proteins.

In addition to the common responses at community level, differences taxa-specific responses were also observed. A substantial reduction in the expression of *kdpA* and *kdpB* encoding a high-affinity K^+ transport system protein that is derived from *Chthoniobacterales* was found. Antimicrobial exposures also resulted in significant decreases of DEGs encoding for carbohydrate transport and metabolism, e.g., transaldolase and glucose-1-phosphate adenylyltransferase. A majority of the downregulated DEGs were derived from *Chthoniobacterales* (23.8 %) and *Rhizobiales* (18.4 %). However, in samples that were treated with the full dosage of glyphosate, *Rhizobiales* downregulated genes that are involved in ABC-type sugar transport systems indicating a specific response toward this antimicrobial substance.

3.6. *Naturally predominant members of the lichen holobiont responded by distinct metabolic adaptions to antimicrobials*

To complement assessments on community-level and deeper investigate different strategies of the bacteria to overcome antimicrobial exposure, one pangenome and three metagenome-assembled genomes (MAGs) were selected for additional analyses. Representative genera of dominant bacterial orders in the lichen microbiome, *i.e.*, *Chthoniobacter* (*Chthoniobacterales*), *Methylobacterium* (*Rhizobiales*), *Granulicella* (*Acidobacteriales*), and *Sphingomonas* (*Sphingomonadales*) were selected. By analyzing their responses using transcriptomic datasets, we observed a congruent trend to the community-level analyses. Clustering in PCoA plots indicated similarities between treated samples, in particular, those that were treated with full dosages of glyphosate and the alkylpyrazine (Fig. S4). The factors explored in this study (antimicrobial type, dosage and their interaction) explained 49.7–60.0 % of the transcriptional variation in the analyzed key taxa. This result indicated a substantial effect of antimicrobial exposure at genus level which is congruent with the observation on community level.

Detailed analysis of transcriptional activity of each key taxon indicated that *Chthoniobacter* significantly downregulated the expression of genes that are involved in energy production in comparison to the control indicating suppression of bacterial metabolic activity. However, genes that are involved in outer membrane lipoprotein and peptidoglycan biosynthesis were upregulated under the full dosage of alkylpyrazine. When the *Sphingomonas*-derived MAGs were assessed in detail, we also observed downregulation of genes involved in energy production, *e.g.*, *ctaC* and *ccoP* that encode cytochrome *C* oxidase subunit II and C-type cytochrome, respectively. Upregulated expression of genes encoding a threonine synthase was also observed upon exposure to all employed antimicrobials. In contrast to other taxa, *Methylobacterium* upregulated expression of genes that encode proteins for energy production and conversion, *e.g.*, glycosyl transferase family 2 and aldehyde oxidase and xanthine dehydrogenase under the full dosages of colistin and glyphosate. In parallel, *Methylobacterium* downregulated *kdA* that encodes a high-affinity K^+ transport system protein; likely to limit

uptake of antimicrobial compounds during the exposure event. Moreover, genes encoding MFS proteins, which also known to confer bacterial drug and multidrug resistance, were highly upregulated under the full dosages of colistin, glyphosate and alkylpyrazine in comparison to untreated control samples. We argue that these regulations could be associated to their resilience towards antimicrobial exposures. *Granulicella* also upregulated expression of gene encoding MFS under the full dosages of glyphosate and alkylpyrazine. Several genes are likely involved to the resilience of this taxon, *e.g.*, carboxypeptidase and sodium solute symporter (SSF) after glyphosate and alkylpyrazine exposure. In addition, *Granulicella* downregulated genes encoding PhoQ sensor in response to all antimicrobials.

3.7. Confirmation of functional responses to antimicrobial exposure by metaproteomics

We employed a metaproteomics approach to further confirm expression of ARGs and to verify observations from the metatranscriptomic data. For these analyses, we selected colistin, a clinical antimicrobial, and alkylpyrazine, a non-clinical antimicrobial. They represent antimicrobials with narrow and broad-spectrum activity, respectively. Most of the detected bacterial proteins in the metaproteomic datasets were assigned to *Rhizobiales, Acidobacteriales*, *Sphingomonadales*, *Caulobacterales,* and *Rhodospiralles* (Fig. 4A-B). This was in line with the DNA-centric analyses. *Rhizobiales, Acidobacteriales*, and *Sphingomonadales* were also the dominant bacterial orders in the lichen microbiome according the 16S rRNA gene fragment amplicon sequencing. The results indicated that antimicrobial treatments substantially affected bacterial protein composition ($P = 0.007$; $R^2 = 0.587$) where samples showed clear tendency to cluster according to the treatment (Fig. S5).

Subsequently, we recovered specific functions that were detected as responses to antimicrobial pressure according to the metatranscriptomic analysis. We focussed on genes within the category "defense mechanisms" (COG V), "cell wall/membrane/envelope biogenesis" (COG M) and "posttranslational modification, protein turnover, chaperones" (COG O). Proteins that are associated with ABC transporters were found to be significantly enriched in antimicrobial-treated samples, in particular alkylpyrazines-treated samples (Table S14). Interestingly, abundances of ABC transporters that are primarily involved in other processes such as amino acid, inorganic ion and carbohydrate transport and metabolism were also increased (Table S15). The findings confirmed that a plethora of ABC transporters naturally occurring in the lichen resistome, was employed as a functional response to first-time antimicrobial exposures. The heat shock 70 kDa protein that was decreased according to the metatranscriptomic analysis followed the same tendency in the metaproteomic approach in the samples treated with alkylpyrazine (Table S14). Membrane proteins, namely Omp2b porin and Ompa motb domain protein that are involved in ion uptake of *Rhizobiales*, *Sphingobacteriales,* and *Rhodospirillales*, were also reduced.

4. Discussion

In this study, our experimental strategy involving different omics technologies and an unusual model system allowed us to explain mechanisms of how chemical exposure alters the functioning of a natural microbiota. Interestingly, bacteria were shown to rely on community-level adaptations during antimicrobial stress after the initial exposure. The observation adds to current knowledge related to resistance development in single strains or in defined biofilms (Davies and Davies 2010). Prevailing adaptions mechanisms at microbiome level were found to be based on the activation of the intrinsic resistome and metabolic adaptation as a trade-off for survival (Fig. 5). At genus level, bacterial members were shown to employ a specific strategy to contribute to the general response.

Interestingly, an unexpectedly high resilience of the bacterial community was found even after continuous exposure to antimicrobial compounds. Exposure to antimicrobials with a broad spectrum activity

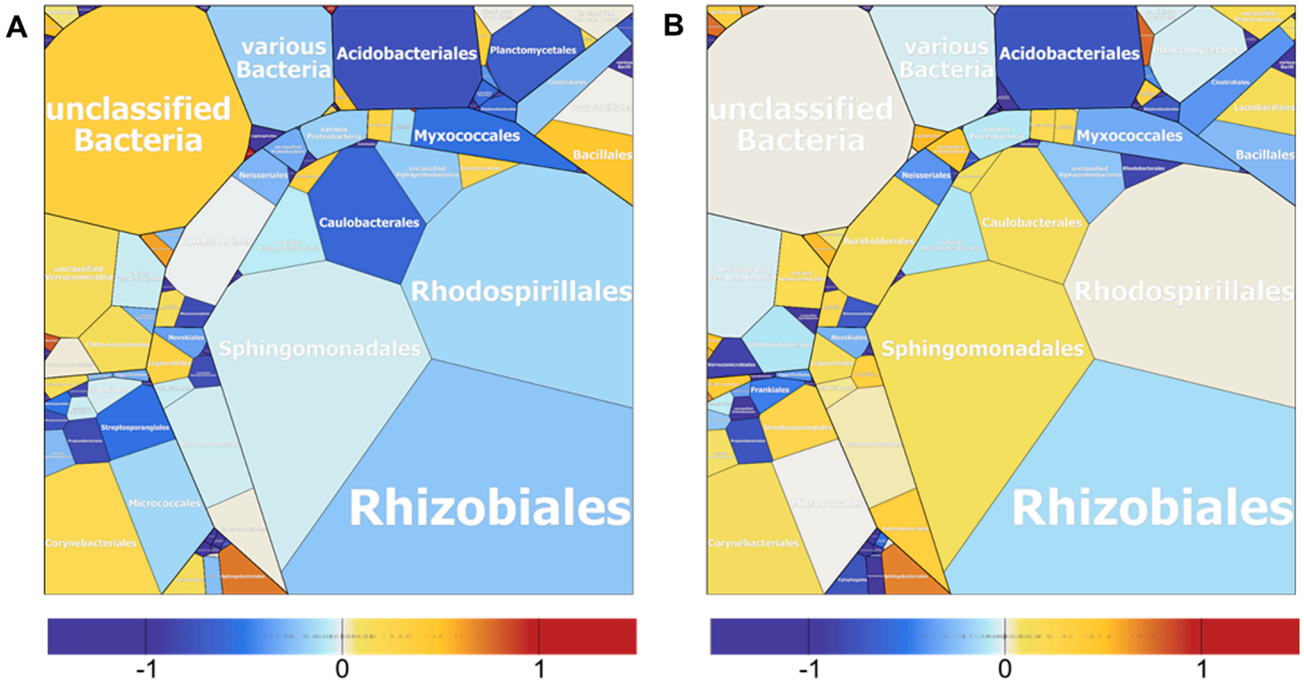

Fig. 4. Voronoi treemap visualization highlighting changes in bacterial metaproteome composition on the bacterial order level. The control versus colistin treatment (A) as well as control versus alkylpyrazine treatment (B) were subjected to direct comparisons. Field sizes represent the relative abundance of the bacterial metaproteome for all conditions (A – control and colistin; B – control and alkylpyrazine). Taxonomic assignments were performed using the analysis pipeline Prophane. For comparison, the $\log_2$-fold change (control/antimicrobial treatment) was used. The colour gradients indicate relative abundance changes of bacterial taxa from low (blue) to high (green) when control and treated samples are compared. (For interpretation of the references to colour in this figure legend, the reader is referred to the web version of this article.)

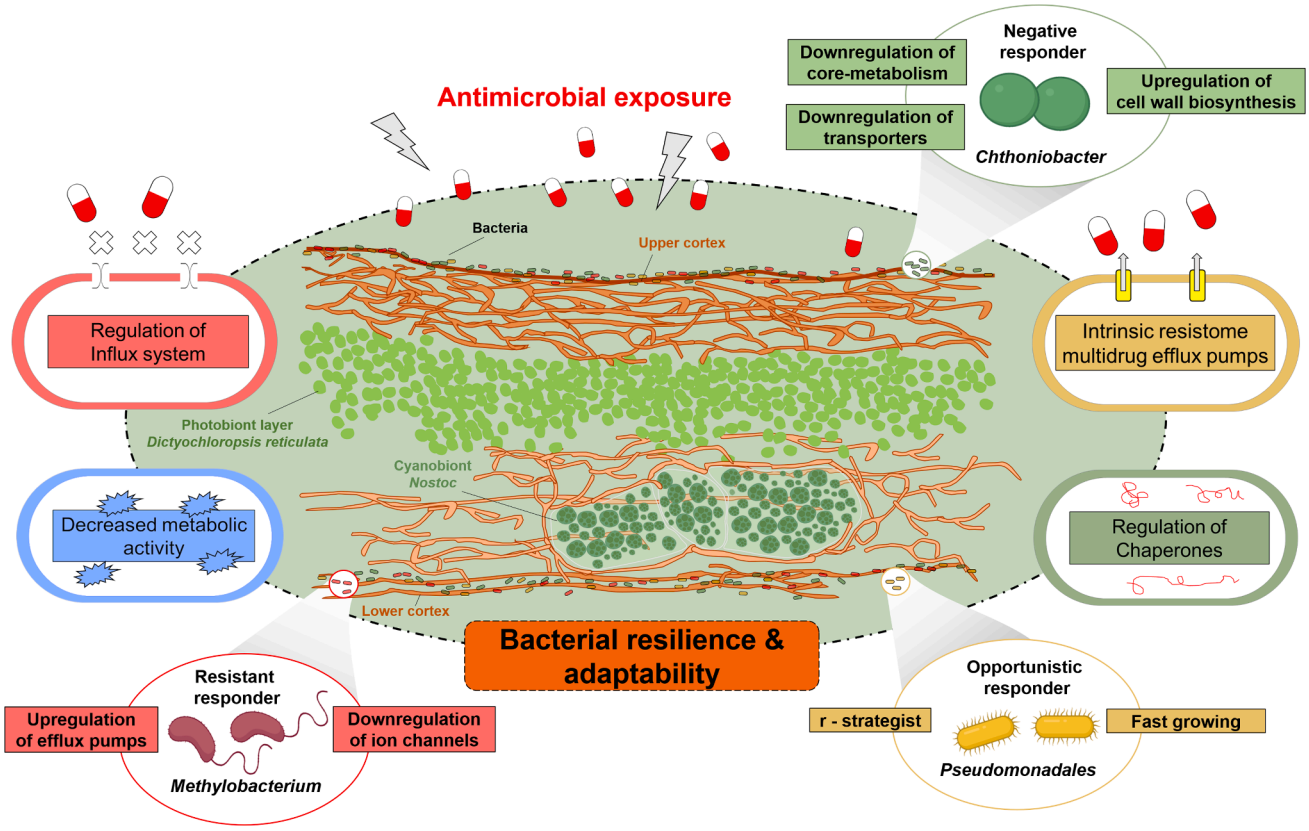

Fig. 5. Schematic illustration of strategies employed by bacteria at community and individual responder level to resist exposure to antimicrobials. The model was constructed on the basis of metatransriptomic and metaproteomic data that were either conducted on the basis of whole datasets or such that specifically targeted distinct lichen microbiome members, i.e., *Methylobacterium*, *Chtoniobacter*, and *Pseudomonadales*.

were previously shown to likely reduce bacterial richness (Raymond et al. 2016; Grenni et al. 2018). However, in the present study bacterial abundance and richness were maintained at comparable levels in all treatments. It is noteworthy to mention that the highest diversity was observed in colistin-treated samples. This is in line with the intermediate disturbance hypothesis which implies that the highest species diversity occurs at intermediate levels of disturbance (Wilkinson 1999; Santillan et al. 2019). Therefore, we hypothesize that colistin, due to its narrow spectrum compared to other antimicrobials used, depleted target species while increasing the abundance of rare taxa previously undetected in untreated samples. Another factor that could explain resilience of lichen-associated bacteria towards antibiotics is prior exposure to antimicrobials. *Lobaria* is known for its diversity of secondary metabolites that are produced to cope with UV radiation and grazing; however, these compounds have different structures and modes of action (Asplund 2011). The long lifespan of lichens also allows for a considerable exposome over time.

The resilience of the microbiota as a whole was linked to antimicrobial-specific shifts in the bacterial community structure with a more profound effect of the non-clinical antimicrobial substances. When these shifts were explored in detail, a reduction of the relative abundance of *Chthoniobacterales* as major contributor to the functional guild in the lichen holobiont (Cernava et al. 2017) was observed. In contrast, *Pseudomonadales* that are considered as "protectors" against pathogens in the lichen holobiont but also in plants, as well as other naturally low abundant taxa thrived under full dosages of glyphosate and the alkylpyrazine. We hypothesize that *Chthoniobacterales* depletion opened niches for *Pseudomonadales,* which are characterized by high metabolic versatility and a r-strategist lifestyle, but also commonly harbour a diverse repertoire of antimicrobial resistance mechanisms (Masák et al. 2014; Banin et al. 2017). Moreover, the heterogeneous group of *Pseudomonadales* can also harbor opportunistic pathogens, e.g., *Pseudomonas aeruginosa*. Hence, the potential for emergence of opportunistic pathogens as the consequence of community disturbance by antimicrobial exposure as previously only shown under build environment or clinical settings (Raymond et al. 2016; O'Hara et al. 2017; Mahnert et al. 2019) was also shown for a natural system.

The overall lichen resistome was characterized by a versatile ARG pool of 26 antibiotic classes anchored in the genome or on plasmids with a dominance of multidrug efflux pumps. They were also identified as the first frontier in the response to all antimicrobial exposures. Efflux pumps are highly conserved and prevalent in environmental microbiomes; they represent an evolutionary old mechanism that is used for detoxification and signalling in bacteria, but also to cope with antimicrobials (Martínez 2008; Martinez et al. 2009). We argue that the rich repertoire of multidrug resistance efflux pumps is required by native bacteria to protect the entire symbiosis against external stressors, to compete with invading microbes, and to survive on the lichen surfaces which is a considerably hostile environment. This also explains the adaptability of major bacterial orders in the model system, including *Rhizobiales* and *Acidobacteriales*, as these taxa actively expressed multidrug resistance efflux pumps, in particular ABC transporter efflux pumps, and resisted antimicrobial exposures.

Unexpectedly, most of the constituents of the intrinsic resistome that were activated under the induced stress were found to be located on bacterial chromosomes and are hence likely involved in other metabolic processes (Martínez 2008; Martínez 2012). Notably, the overexpression of ARGs was followed by distinct consequences, mainly by down-regulation of key transcriptional activities, *e.g.*, energy production and conversion, carbohydrate transport and metabolism, inorganic ion transport and metabolism that were observed at RNA and protein levels. This finding provides the first community-level confirmation for a trade-

off between antimicrobial resistance and biological fitness as survival strategy of bacterial communities under antimicrobial exposure. It was identified as general mode of action towards all antimicrobials at community level. Similar phenomena were previously found with single strains (Kang and Park 2010; Balaban 2011; Martínez and Rojo 2011; Phan and Ferenci 2017). We suggest that the decrease of key metabolic activity is a result of decreased influx system activity to limit uptake of antimicrobial substances. This regulation strategy is commonly found in pathogenic Gram-negative bacteria as an adaptation in response to antimicrobial exposure (Pagès et al. 2008). Moreover, a reduced chaperone expression which is required for correct folding of protein during biosynthesis peaks and heat stress (Junttila et al. 2013; Carniel et al. 2016) was observed. Chaperones were previously shown to be activated by the lichen microbiota upon exposure to constant oxidative and osmotic stress (Cernava et al. 2019). The regulation of chaperones under antimicrobial stress provides further evidence for the adaptability of the lichen community and might be connected to its survival strategy. We argue that the upregulation of multidrug efflux pumps imposes substantial energy costs on the lichen microbiota. As a trade-off, the lichen microbiota down-regulates the expression of chaperones that are likely not required for coping with the antimicrobials that were applied.

The general response of the lichen microbiota to antimicrobials was assessed at quantitative and qualitative levels. We observed that the number of differentially expressed bacterial genes, gradually increased for colistin < tetracycline < alkylpyrazine < glyphosate. Differences in the activity spectrum of antimicrobial substances may have caused divergent effects on transcription activity of the lichen holobiont. We therefore assume that the exposure to glyphosate and alkylpyrazine resulted in a more profound transcriptional response due to the involvement of eukaryotic partners in contrast to the tetracycline and colistin treatments. The general response mechanism was deciphered for bacterial key taxa as well.

Targeted analyses of key taxa based on metagenome-assembled genomes reflected the community-level responses but also revealed diversified strategies of their players (Fig. 5). *Chthoniobacter* was shown to be comparatively less equipped with an intrinsic resistome, thus downregulation of genes encoding transporter proteins is likely employed to limit antimicrobial compounds entering the cell. This was also followed by downregulation of genes related to energy conversion which finally limited the growth of *Chthoniobacter* as the negative responder (Fig. 5). *Methylobacterium*, as a resistant responder, also followed the first strategy (Fig. 5) but simultaneously upregulated expression of major facilitator superfamily (MFS) proteins. MFS proteins are used to transport a various substrates across membranes and play a key role in various physiological processes including symbiotic interactions between *Rhizobiales* and their plant hosts (Yan 2013; Pasqua et al. 2019). These proteins are also considered as a crucial elements that contribute to drug resistance in bacteria (Gibson et al. 2015; Pasqua et al. 2019). Interestingly, *Granulicella* (*Acidobacteriales*) also upregulated an analogous gene and simultaneously downregulated the PhoQ sensor, a part a two-component regulatory system, which plays a key role in specific bacterial resistance to polymyxin B and antimicrobial peptides (Gooderham and Hancock 2009). Hence, we hypothesize that these resistance mechanisms were deactivated in favour of the more needed multidrug efflux systems. Here, regulation of key genes in *Methylobacterium* and *Granulicella* likely represents an initial strategy for resilience enhancement under the induced stress. We observed a consistence in the reduced expression of ferritin-like proteins by *Sphingomonadales*, *Sphingobacteriales*, *Acidobacteriales,* and *Rhizobiales* under the full dosage of the employed antimicrobials. Iron storage proteins are known to suppress resistance evolution and adaption of bacteria toward lethal dosages of antimicrobial substances (Méhi et al. 2014), thus our observation indicates a simultaneous deactivation of this mechanism to facilitate resistance formation in key players of the lichen holobiont.

AMR emergence poses a substantial threat to human health. Considering WHO's One Health concept, lichens are an important but so far neglected reservoir for AMR. The four most important criteria to determine the risk of AMR emergence from sequence data are if they are i) complete, potential functional signatures, ii) linked with other resistances, iii) mobile and iv) associated to hosts (Qian et al. 2021). We have shown that lichens harbour functional ARGs and mobile genetic elements encoding AMR; both were expressed at RNA and protein level. Although mainly non-mobile ARGs were activated during antimicrobial pressure, they can be transferred by horizontal gene transfer. Lichens represent a substantial biological surface area on Earth and are embedded in food cycles, e.g. they are the main food for reindeers being the most numerous large herbivores in circumpolar areas (Bernes et al. 2015). In the future, a careful assessment will be essential to determine the risk of AMR spread from these widespread organisms.

In conclusion, our results suggest that at lichen microbiota level, a trade-off between antimicrobial resistance and biological fitness can be employed as survival strategy under antimicrobial exposure. The first defence line, including activation of the intrinsic resistance repertoire and reduction of bacterial metabolic activity, limits the uptake of antimicrobial substances while subsequent mechanisms provide prolonged protection. The long-term protection strategies employed by the bacterial community likely involve accelerated resistance development as a survival strategy. We hypothesize that the phenomena observed in the lichen microbiome, representative for a well-defined micro-ecosystem, reflect potential large-scale responses when natural systems encounter exposure to antibiotics.

Declaration of Competing Interest

The authors declare that they have no known competing financial interests or personal relationships that could have appeared to influence the work reported in this paper.

Data availability

Sequencing data for each sample used in this study was deposited at the European Nucleotide Archive (ENA) in the FASTQ format.

Acknowledgements

We want to thank Adriana Attanassova, Christian Berg and Martin Grube (Graz) for their help during the lichen sampling. We also want to thank Sabine Erschen and Barbara Fetz (Graz) for their support during DNA extractions and sample preparations. Graphic elements for Fig. 5 were obtained from BioRender (https://biorender.com/). This study was supported by a grant from the FWF (Austrian Science Fund) and the federal state government of Styria to G.B. (P29285-BBL).

Ethics approval and consent to participate

Not applicable.

Data and materials availability

Sequencing data for each sample used in this study was deposited at the European Nucleotide Archive (ENA) in the FASTQ format and is available under the Bioproject accession number PRJEB48781 for amplicon sequencing dataset, PRJEB38505 for metagenome dataset and PRJEB48783 for metatransciptome dataset.

Author's Contributions

GB, TC, and WAW conceived and designed the study. WAW, and MB performed the experiment. WAW performed bioinformatic analysis. WAW, TC, and GB wrote the manuscript. WAW, TC, MB, and JB analyzed the data. WAW, TC, GB, MB, JB, and KR critically read and commented on the manuscript. All authors have read and agreed to the

published version of the manuscript.

Appendix A. Supplementary material

Supplementary data to this article can be found online at https://doi.org/10.1016/j.envint.2022.107474.

References

Ahmadjian, V., 1995. Lichens are more important than you think. Bioscience 45 (3), 124.

Alneberg, J., Bjarnason, B.S., de Bruijn, I., Schirmer, M., Quick, J., Ijaz, U.Z., Lahti, L., Loman, N.J., Andersson, A.F., Quince, C., 2014. Binning metagenomic contigs by coverage and composition. Nat. Methods 11 (11), 1144–1146.

Arango-Argoty, G., Garner, E., Pruden, A., Heath, L.S., Vikesland, P., Zhang, L., 2018. DeepARG: a deep learning approach for predicting antibiotic resistance genes from metagenomic data. Microbiome. 6 (1), 1–15.

Asplund, J., 2011. Chemical races of Lobaria pulmonaria differ in palatability to gastropods. Lichenologist 43 (5), 491–494.

Balaban, N.Q., 2011. Persistence: mechanisms for triggering and enhancing phenotypic variability. Curr. Opin. Genet. Dev. 21 (6), 768–775.

Banin, E., Hughes, D., Kuipers, O.P., 2017. Bacterial pathogens, antibiotics and antibiotic resistance. FEMS Microbiol. Rev. 41 (3), 450–452.

Berbee, M.L., Strullu-Derrien, C., Delaux, P.-M., Strother, P.K., Kenrick, P., Selosse, M.-A., Taylor, J.W., 2020. Genomic and fossil windows into the secret lives of the most ancient fungi. Nat. Rev. Microbiol. 18 (12), 717–730.

Berendonk, T.U., Manaia, C.M., Merlin, C., Fatta-Kassinos, D., Cytryn, E., Walsh, F., Bürgmann, H., Sørum, H., Norström, M., Pons, M.-N., Kreuzinger, N., Huovinen, P., Stefani, S., Schwartz, T., Kisand, V., Baquero, F., Martinez, J.L., 2015. Tackling antibiotic resistance: the environmental framework. Nat. Rev. Microbiol. 13 (5), 310–317.

Berg, G., Rybakova, D., Fischer, D., Cernava, T., Vergès, M.-C.-C., Charles, T., Chen, X., Cocolin, L., Eversole, K., Corral, G.H., 2020. Microbiome definition re-visited: old concepts and new challenges. Microbiome 8 (1), 1–22.

Bernes, C., Bråthen, K.A., Forbes, B.C., Speed, J.D., Moen, J., 2015. What are the impacts of reindeer/caribou (Rangifer tarandus L.) on arctic and alpine vegetation? A systematic review. Environ Evid. 4 (1), 1–26.

Bernhardt, E.S., Rosi, E.J., Gessner, M.O., 2017. Synthetic chemicals as agents of global change. Front. Ecol. Environ. 15 (2), 84–90.

Bolger, A.M., Lohse, M., Usadel, B., 2014. Trimmomatic: a flexible trimmer for Illumina sequence data. Bioinformatics 30 (15), 2114–2120.

Bolyen, E., Rideout, J.R., Dillon, M.R., Bokulich, N.A., Abnet, C.C., Al-Ghalith, G.A., Alexander, H., Alm, E.J., Arumugam, M., Asnicar, F., Bai, Y., Bisanz, J.E., Bittinger, K., Brejnrod, A., Brislawn, C.J., Brown, C.T., Callahan, B.J., Caraballo-Rodríguez, A.M., Chase, J., Cope, E.K., Da Silva, R., Diener, C., Dorrestein, P.C., Douglas, G.M., Durall, D.M., Duvallet, C., Edwardson, C.F., Ernst, M., Estaki, M., Fouquier, J., Gauglitz, J.M., Gibbons, S.M., Gibson, D.L., Gonzalez, A., Gorlick, K., Guo, J., Hillmann, B., Holmes, S., Holste, H., Huttenhower, C., Huttley, G.A., Janssen, S., Jarmusch, A.K., Jiang, L., Kaehler, B.D., Kang, K.B., Keefe, C.R., Keim, P., Kelley, S.T., Knights, D., Koester, I., Kosciolek, T., Kreps, J., Langille, M.G.I., Lee, J., Ley, R., Liu, Y.-X., Loftfield, E., Lozupone, C., Maher, M., Marotz, C., Martin, B.D., McDonald, D., McIver, L.J., Melnik, A.V., Metcalf, J.L., Morgan, S.C., Morton, J.T., Naimey, A.T., Navas-Molina, J.A., Nothias, L.F., Orchanian, S.B., Pearson, T., Peoples, S.L., Petras, D., Preuss, M.L., Pruesse, E., Rasmussen, L.B., Rivers, A., Robeson, M.S., Rosenthal, P., Segata, N., Shaffer, M., Shiffer, A., Sinha, R., Song, S.J., Spear, J.R., Swafford, A.D., Thompson, L.R., Torres, P.J., Trinh, P., Tripathi, A., Turnbaugh, P.J., Ul-Hasan, S., van der Hooft, J.J.J., Vargas, F., Vázquez-Baeza, Y., Vogtmann, E., von Hippel, M., Walters, W., Wan, Y., Wang, M., Warren, J., Weber, K. C., Williamson, C.H.D., Willis, A.D., Xu, Z.Z., Zaneveld, J.R., Zhang, Y., Zhu, Q., Knight, R., Caporaso, J.G., 2019. Reproducible, interactive, scalable and extensible microbiome data science using QIIME 2. Nat. Biotechnol. 37 (8), 852–857.

Bottery, M.J., Pitchford, J.W., Friman, V.-P., 2021. Ecology and evolution of antimicrobial resistance in bacterial communities. ISME J.:1–10. 15 (4), 939–948.

Brealey, J.C., Leitão, H.G., van der Valk, T., Xu, W., Bougiouri, K., Dalén, L., Guschanski, K., Falush, D., 2020. Dental calculus as a tool to study the evolution of the mammalian oral microbiome. Mol. Biol. Evol. 37 (10), 3003–3022.

Callahan, B.J., McMurdie, P.J., Rosen, M.J., Han, A.W., Johnson, A.J.A., Holmes, S.P., 2016. DADA2: high-resolution sample inference from Illumina amplicon data. Nat. Methods 13 (7), 581–583.

Caniaux, I., van Belkum, A., Zambardi, G., Poirel, L., Gros, M.F., 2017. MCR: modern colistin resistance. Eur. J. Clin. Microbiol. Infect. Dis. 36 (3), 415–420.

Carniel, F.C., Gerdol, M., Montagner, A., Banchi, E., De Moro, G., Manfrin, C., Muggia, L., Pallavicini, A., Tretiach, M., 2016. New features of desiccation tolerance in the lichen photobiont Trebouxia gelatinosa are revealed by a transcriptomic approach. Plant Mol. Biol. 91 (3), 319–339.

Cernava, T., Erlacher, A., Aschenbrenner, I.A., Krug, L., Lassek, C., Riedel, K., Grube, M., Berg, G., 2017. Deciphering functional diversification within the lichen microbiota by meta-omics. Microbiome. 5 (1), 82.

Cernava, T., Vasfiu, Q., Erlacher, A., Aschenbrenner, I.A., Francesconi, K., Grube, M., Berg, G., 2018. Adaptions of lichen microbiota functioning under persistent exposure to arsenic contamination. Front. Microbiol. 9, 2959.

Cernava, T., Aschenbrenner, I.A., Soh, J., Sensen, C.W., Grube, M., Berg, G., 2019. Plasticity of a holobiont: desiccation induces fasting-like metabolism within the lichen microbiota. ISME J. 13 (2), 547–556.

Chong, J., Liu, P., Zhou, G., Xia, J., 2020. Using MicrobiomeAnalyst for comprehensive statistical, functional, and meta-analysis of microbiome data. Nat. Protoc.:1–23.

Collignon, P.C., Conly, J.M., Andremont, A., McEwen, S.A., Aidara-Kane, A., Griffin, P. M., 2016. World Health Organization ranking of antimicrobials according to their importance in human medicine: a critical step for developing risk management strategies to control antimicrobial resistance from food animal production. Clin. Infect. Dis. 63 (8), 1087–1093.

Davies, J., Davies, D., 2010. Origins and evolution of antibiotic resistance. Microbiol. Mol. Biol. Rev. 74 (3), 417–433.

FAOSTAT. 2021. Pesticides Use. [accessed 2022 Jan 12]. https://www.fao.org/faostat/en/#data/RP.

Gibson, M.K., Forsberg, K.J., Dantas, G., 2015. Improved annotation of antibiotic resistance determinants reveals microbial resistomes cluster by ecology. ISME J. 9 (1), 207–216.

Gooderham, W.J., Hancock, R.E.W., 2009. Regulation of virulence and antibiotic resistance by two-component regulatory systems in Pseudomonas aeruginosa. FEMS Microbiol. Rev. 33 (2), 279–294.

Grenni, P., Ancona, V., Barra Caracciolo, A., 2018. Ecological effects of antibiotics on natural ecosystems: a review. Microchem. J. 136, 25–39.

Grube, M., Cernava, T., Soh, J., Fuchs, S., Aschenbrenner, I., Lassek, C., Wegner, U., Becher, D., Riedel, K., Sensen, C.W., Berg, G., 2015. Exploring functional contexts of symbiotic sustain within lichen-associated bacteria by comparative omics. ISME J. 9 (2), 412–424.

Huerta-Cepas, J., Forslund, K., Coelho, L.P., Szklarczyk, D., Jensen, L.J., Von Mering, C., Bork, P., 2017. Fast genome-wide functional annotation through orthology assignment by eggNOG-mapper. Mol. Biol. Evol. 34 (8), 2115–2122.

Huerta-Cepas, J., Szklarczyk, D., Heller, D., Hernández-Plaza, A., Forslund, S.K., Cook, H., Mende, D.R., Letunic, I., Rattei, T., Jensen, L.J., 2019. eggNOG 5.0: a hierarchical, functionally and phylogenetically annotated orthology resource based on 5090 organisms and 2502 viruses. Nucleic Acids Res. 47 (D1), D309–D314.

Hyatt, D., Chen, G.-L., LoCascio, P.F., Land, M.L., Larimer, F.W., Hauser, L.J., 2010. Prodigal: prokaryotic gene recognition and translation initiation site identification. BMC Bioinf. 11 (1), 119.

Junttila, S., Laiho, A., Gyenesei, A., Rudd, S., 2013. Whole transcriptome characterization of the effects of dehydration and rehydration on Cladonia rangiferina, the grey reindeer lichen. BMC Genomics 14 (1), 870. https://doi.org/10.1186/1471-2164-14-870.

Kang, D.D., Li, F., Kirton, E., Thomas, A., Egan, R., An, H., Wang, Z., 2019. MetaBAT 2: an adaptive binning algorithm for robust and efficient genome reconstruction from metagenome assemblies. PeerJ 7, e7359.

Kang, Y., Park, W., 2010. Trade-off between antibiotic resistance and biological fitness in Acinetobacter sp. strain DR1. Environ. Microbiol. 12 (5), 1304–1318.

Krawczyk, P.S., Lipinski, L., Dziembowski, A., 2018. PlasFlow: predicting plasmid sequences in metagenomic data using genome signatures. Nucleic Acids Res. 46 (6), e35.

Krug, L., Erlacher, A., Berg, G., Cernava, T., 2019. A novel, nature-based alternative for photobioreactor decontaminations. Sci. Rep. 9 (1), 1–10.

Kusstatscher, P., Cernava, T., Liebminger, S., Berg, G., 2017. Replacing conventional decontamination of hatching eggs with a natural defense strategy based on antimicrobial, volatile pyrazines. Sci. Rep. 7 (1), 1–8.

Laing, C., Buchanan, C., Taboada, E.N., Zhang, Y., Kropinski, A., Villegas, A., Thomas, J. E., Gannon, V.P., 2010. Pan-genome sequence analysis using Panseq: an online tool for the rapid analysis of core and accessory genomic regions. BMC Bioinf. 11 (1), 461.

Langmead, B., Salzberg, S.L., 2012. Fast gapped-read alignment with Bowtie 2. Nat. Methods 9 (4), 357–359.

Li, H., Durbin, R., 2010. Fast and accurate long-read alignment with Burrows-Wheeler transform. Bioinformatics 26 (5), 589–595.

Li, J., Nation, R.L., Turnidge, J.D., Milne, R.W., Coulthard, K., Rayner, C.R., Paterson, D. L., 2006. Colistin: the re-emerging antibiotic for multidrug-resistant Gram-negative bacterial infections. Lancet Infect. Dis. 6 (9), 589–601.

Liao, H., Li, X.i., Yang, Q., Bai, Y., Cui, P., Wen, C., Liu, C., Chen, Z., Tang, J., Che, J., Yu, Z., Geisen, S., Zhou, S., Friman, V.-P., Zhu, Y.-G., Falush, D., 2021. Herbicide selection promotes antibiotic resistance in soil microbiomes. Mol. Biol. Evol. 38 (6), 2337–2350.

Liao, Y., Smyth, G.K., Shi, W., 2014. featureCounts: an efficient general purpose program for assigning sequence reads to genomic features. Bioinformatics 30 (7), 923–930.

Liu, Z., Klümper, U., Liu, Y., Yang, Y., Wei, Q., Lin, J.-G., Gu, J.-D., Li, M., 2019. Metagenomic and metatranscriptomic analyses reveal activity and hosts of antibiotic resistance genes in activated sludge. Environ. Int. 129, 208–220.

Looft, T., Johnson, T.A., Allen, H.K., Bayles, D.O., Alt, D.P., Stedtfeld, R.D., Sul, W.J., Stedtfeld, T.M., Chai, B., Cole, J.R., 2012. In-feed antibiotic effects on the swine intestinal microbiome. Proc. Natl. Acad. Sci. 109 (5), 1691–1696.

Love, M.I., Huber, W., Anders, S., 2014. Moderated estimation of fold change and dispersion for RNA-seq data with DESeq2. Genome Biol. 15 (12), 550.

Mahnert, A., Moissl-Eichinger, C., Zojer, M., Bogumil, D., Mizrahi, I., Rattei, T., Martinez, J.L., Berg, G., 2019. Man-made microbial resistances in built environments. Nat. Commun. 10 (1), 1–12.

Martínez, J.L., 2008. Antibiotics and antibiotic resistance genes in natural environments. Science 321 (5887), 365–367.

Martínez, J.L., 2012. Natural antibiotic resistance and contamination by antibiotic resistance determinants: the two ages in the evolution of resistance to antimicrobials. Front. Microbiol. 3, 1.

Martínez, J.L., Rojo, F., 2011. Metabolic regulation of antibiotic resistance. FEMS Microbiol. Rev. 35 (5), 768–789.

Martinez, J.L., Sánchez, M.B., Martínez-Solano, L., Hernandez, A., Garmendia, L., Fajardo, A., Alvarez-Ortega, C., 2009. Functional role of bacterial multidrug efflux pumps in microbial natural ecosystems. FEMS Microbiol. Rev. 33 (2), 430–449.
Masák, J., Čejková, A., Schreiberová, O., Rezanka, T., 2014. Pseudomonas biofilms: possibilities of their control. FEMS Microbiol. Ecol. 89 (1), 1–14.
Mbanaso, F.U., Coupe, S.J., Charlesworth, S.M., Nnadi, E.O., 2013. Laboratory-based experiments to investigate the impact of glyphosate-containing herbicide on pollution attenuation and biodegradation in a model pervious paving system. Chemosphere 90 (2), 737–746.
McDonald, D., Price, M.N., Goodrich, J., Nawrocki, E.P., DeSantis, T.Z., Probst, A., Andersen, G.L., Knight, R., Hugenholtz, P., 2012. An improved Greengenes taxonomy with explicit ranks for ecological and evolutionary analyses of bacteria and archaea. ISME J. 6 (3), 610–618.
McMurdie, P.J., Holmes, S., Watson, M., 2013. phyloseq: an R package for reproducible interactive analysis and graphics of microbiome census data. PLoS ONE 8 (4).
Méhi, O., Bogos, B., Csörgő, B., Pál, F., Nyerges, Á., Papp, B., Pál, C., 2014. Perturbation of iron homeostasis promotes the evolution of antibiotic resistance. Mol. Biol. Evol. 31 (10), 2793–2804.
Menzel, P., Ng, K.L., Krogh, A., 2016. Fast and sensitive taxonomic classification for metagenomics with Kaiju. Nat. Commun. 7 (1), 1–9.
Murray, C.J., Ikuta, K.S., Sharara, F., Swetschinski, L., Aguilar, G.R., Gray, A., Han, C., Bisignano, C., Rao, P., Wool, E., 2022. Global burden of bacterial antimicrobial resistance in 2019: a systematic analysis. Lancet.
Nurk, S., Meleshko, D., Korobeynikov, A., Pevzner, P.A., 2017. metaSPAdes: a new versatile metagenomic assembler. Genome Res. 27 (5), 824–834.
O'Hara, N.B., Reed, H.J., Afshinnekoo, E., Harvin, D., Caplan, N., Rosen, G., Frye, B., Woloszynek, S., Ounit, R., Levy, S., Butler, E., Mason, C.E., 2017. Metagenomic characterization of ambulances across the USA. Microbiome. 5 (1) https://doi.org/10.1186/s40168-017-0339-6.
Obermeier, M.M., Wicaksono, W.A., Taffner, J., Bergna, A., Poehlein, A., Cernava, T., Lindstaedt, S., Lovric, M., Müller Bogotá, C.A., Berg, G., 2021. Plant resistome profiling in evolutionary old bog vegetation provides new clues to understand emergence of multi-resistance. ISME J. 15 (3), 921–937.
Oksanen, J., Kindt, R., Legendre, P., O'Hara, B., Stevens, M.H.H., Oksanen, M.J., Suggests, M., 2007. The vegan package. Community Ecol Package 10, 631–637.
Pagès, J.-M., James, C.E., Winterhalter, M., 2008. The porin and the permeating antibiotic: a selective diffusion barrier in Gram-negative bacteria. Nat. Rev. Microbiol. 6 (12), 893–903.
Parada, A.E., Needham, D.M., Fuhrman, J.A., 2016. Every base matters: assessing small subunit rRNA primers for marine microbiomes with mock communities, time series and global field samples. Environ. Microbiol. 18 (5), 1403–1414.
Park, J., Gasparrini, A.J., Reck, M.R., Symister, C.T., Elliott, J.L., Vogel, J.P., Wencewicz, T.A., Dantas, G., Tolia, N.H., 2017. Plasticity, dynamics, and inhibition of emerging tetracycline resistance enzymes. Nat. Chem. Biol. 13 (7), 730–736.
Parks, D.H., Imelfort, M., Skennerton, C.T., Hugenholtz, P., Tyson, G.W., 2015. CheckM: assessing the quality of microbial genomes recovered from isolates, single cells, and metagenomes. Genome Res. 25 (7), 1043–1055.
Pasqua, M., Grossi, M., Zennaro, A., Fanelli, G., Micheli, G., Barras, F., Colonna, B., Prosseda, G., 2019. The Varied Role of Efflux Pumps of the MFS Family in the Interplay of Bacteria with Animal and Plant Cells. Microorganisms. 7 (9), 285.
Paterson, D.L., Harris, P.N.A., 2016. Colistin resistance: a major breach in our last line of defence. Lancet Infect. Dis. 16 (2), 132–133.
Persson, L., Carney Almroth, B.M., Collins, C.D., Cornell, S., de Wit, C.A., Diamond, M.L., Fantke, P., Hassellöv, M., MacLeod, M., Ryberg, M.W., Søgaard Jørgensen, P., Villarrubia-Gómez, P., Wang, Z., Hauschild, M.Z., 2022. Outside the safe operating space of the planetary boundary for novel entities. Environ. Sci. Technol. 56 (3), 1510–1521.
Phan, K., Ferenci, T., 2017. The fitness costs and trade-off shapes associated with the exclusion of nine antibiotics by OmpF porin channels. ISME J. 11 (6), 1472–1482.
Pruesse, E., Quast, C., Knittel, K., Fuchs, B.M., Ludwig, W., Peplies, J., Glöckner, F.O., 2007. SILVA: a comprehensive online resource for quality checked and aligned ribosomal RNA sequence data compatible with ARB. Nucleic Acids Res. 35 (21), 7188–7196.
Qian, X., Gunturu, S., Sun, W., Cole, J.R., Norby, B.o., Gu, J., Tiedje, J.M., 2021. Long-read sequencing revealed cooccurrence, host range, and potential mobility of antibiotic resistome in cow feces. Proc. Natl. Acad. Sci. 118 (25) https://doi.org/10.1073/pnas.2024464118.
Ramakrishnan, B., Venkateswarlu, K., Sethunathan, N., Megharaj, M., 2019. Local applications but global implications: Can pesticides drive microorganisms to develop antimicrobial resistance? Sci. Total Environ. 654, 177–189.
Raymond, F., Ouameur, A.A., Déraspe, M., Iqbal, N., Gingras, H., Dridi, B., Leprohon, P., Plante, P.-L., Giroux, R., Bérubé, È., Frenette, J., Boudreau, D.K., Simard, J.-L., Chabot, I., Domingo, M.-C., Trottier, S., Boissinot, M., Huletsky, A., Roy, P.H., Ouellette, M., Bergeron, M.G., Corbeil, J., 2016. The initial state of the human gut microbiome determines its reshaping by antibiotics. ISME J. 10 (3), 707–720.
Rognes, T., Flouri, T., Nichols, B., Quince, C., Mahé, F., 2016. VSEARCH: a versatile open source tool for metagenomics. PeerJ 4, e2584.
Santillan, E., Seshan, H., Constancias, F., Drautz-Moses, D.I., Wuertz, S., 2019. Frequency of disturbance alters diversity, function, and underlying assembly mechanisms of complex bacterial communities. npj Biofilms Microbiomes 5 (1), 1–9.
Schiebenhoefer, H., Schallert, K., Renard, B.Y., Trappe, K., Schmid, E., Benndorf, D., Riedel, K., Muth, T., Fuchs, S., 2020. A complete and flexible workflow for metaproteomics data analysis based on MetaProteomeAnalyzer and Prophane. Nat. Protoc. 15 (10), 3212–3239.
Semedo, M., Song, B., Sparrer, T., Phillips, R.L., 2018. Antibiotic effects on microbial communities responsible for denitrification and N2O production in grassland soils. Front. Microbiol. 9, 2121.
Sieber, C.M.K., Probst, A.J., Sharrar, A., Thomas, B.C., Hess, M., Tringe, S.G., Banfield, J. F., 2018. Recovery of genomes from metagenomes via a dereplication, aggregation and scoring strategy. Nat. Microbiol. 3 (7), 836–843.
Søgaard Jørgensen, P., Aktipis, A., Brown, Z., Carriere, Y., Downes, S., Dunn, R.R., Epstein, G., Frisvold, G.B., Hawthorne, D., Grohn, Y.T., 2018. Antibiotic and pesticide susceptibility and the Anthropocene operating space. Nat Sustain. 1 (11), 632–641.
Steffen, W., Broadgate, W., Deutsch, L., Gaffney, O., Ludwig, C., 2015. The trajectory of the Anthropocene: the great acceleration. Anthr Rev. 2 (1), 81–98.
Stewart, F.J., Ottesen, E.A., DeLong, E.F., 2010. Development and quantitative analyses of a universal rRNA-subtraction protocol for microbial metatranscriptomics. ISME J. 4 (7), 896–907.
Unep, 2019. Global Chemicals Outlook II-From Legacies to Innovative Solutions. Implementing the 2030 Agenda for Sustainable Development.
Van Boeckel, T.P., Brower, C., Gilbert, M., Grenfell, B.T., Levin, S.A., Robinson, T.P., Teillant, A., Laxminarayan, R., 2015. Global trends in antimicrobial use in food animals. Proc. Natl. Acad. Sci. 112 (18), 5649–5654.
Van Goethem, M.W., Pierneef, R., Bezuidt, O.K., Van De Peer, Y., Cowan, D.A., Makhalanyane, T.P., 2018. A reservoir of 'historical'antibiotic resistance genes in remote pristine Antarctic soils. Microbiome 6 (1), 40.
Vermeulen, R., Schymanski, E.L., Barabási, A.-L., Miller, G.W., 2020. The exposome and health: Where chemistry meets biology. Science 367 (6476), 392–396.
von Meijenfeldt, F.B., Arkhipova, K., Cambuy, D.D., Coutinho, F.H., Dutilh, B.E., 2019. Robust taxonomic classification of uncharted microbial sequences and bins with CAT and BAT. Genome Biol. 20 (1), 217.
Vorholt, J.A., 2012. Microbial life in the phyllosphere. Nat. Rev. Microbiol. 10 (12), 828–840.
Wang, W., Vignani, R., Scali, M., Cresti, M., 2006. A universal and rapid protocol for protein extraction from recalcitrant plant tissues for proteomic analysis. Electrophoresis 27 (13), 2782–2786.
Wicaksono, W.A., Kusstatscher, P., Erschen, S., Reisenhofer-Graber, T., Grube, M., Cernava, T., Berg, G., 2021. Antimicrobial-specific response from resistance gene carriers studied in a natural, highly diverse microbiome. Microbiome. 9 (1), 1–14.
Wild, C.P., 2005. Complementing the genome with an "exposome": the outstanding challenge of environmental exposure measurement in molecular epidemiology. Cancer Epidemiol Prev Biomark. 14 (8), 1847–1850.
Wilkinson, D.M., 1999. The disturbing history of intermediate disturbance. Oikos 84 (1), 145. https://doi.org/10.2307/3546874.
World Health Organization, 2021. Antimicrobial resistance and the United Nations sustainable development cooperation framework: guidance for United Nations country teams.
Wu, Y.-W., Simmons, B.A., Singer, S.W., 2016. MaxBin 2.0: an automated binning algorithm to recover genomes from multiple metagenomic datasets. Bioinformatics 32 (4), 605–607.
Yan, N., 2013. Structural advances for the major facilitator superfamily (MFS) transporters. Trends Biochem. Sci. 38 (3), 151–159.
Ye, G., Qiu, Y., He, X., Zhao, L., Shi, F., Lv, C., Jing, B., Li, Y., 2015. Effect of two macrocephala flavored powder supplementation on intestinal morphology and intestinal microbiota in weaning pigs. Int. J. Clin. Exp. Med. 8 (1), 1504.